Soft mode-driven reduction of switching energy barriers in fluorite ferroelectric

Jinhyeong Jo,[1,*] Pawan Kumar,[1,*] and Jun Hee Lee[1,2,†]
[1]Department of Energy Engineering, School of Energy and Chemical Engineering, UNIST, Ulsan 44919, Republic of Korea
[2]Graduate School of Semiconductor Materials and Devices Engineering, UNIST, Ulsan 44919, Republic of Korea

(Received 5 May 2025; accepted 15 September 2025; published 14 October 2025)

The low coercive field (E_c) is highly desirable for developing efficient and durable ferroelectric-based devices. However, fluorite ferroelectrics such as HfO_2 and ZrO_2, which are attracting significant attention as next-generation semiconductor materials due to their compatibility with complementary metal-oxide-semiconductor technology and robust ferroelectric properties, exhibit a significantly high E_c, severely limiting their application in memory devices. Here, using group theory and first-principles simulations, we reveal that phonon engineering can induce a new soft mode in the polar $Pca2_1$ phase of HfO_2 and ZrO_2. This mode dominates the intermediate transition state during polarization switching and drastically reduces the energy barriers for both homogeneous switching and the uniquely observed local switching, which enables ultrahigh memory density. Furthermore, the discovery of a ternary state during local switching points to the possibility of implementing ternary logic at the material level. Our findings introduce a new pathway to lowering E_c in fluorite ferroelectrics by exploiting intrinsic lattice dynamics, offering an alternative to conventional strategies such as doping or defect engineering, and open a promising direction for future material design.

DOI: 10.1103/kkk8-s3lk

I. INTRODUCTION

The rapid advancement of information and communication technologies, such as artificial intelligence, the Internet of Things, and cloud and edge computing, has increased the demand for faster, more efficient, and higher-capacity memory solutions [1]. This demand has driven the development of new memory architectures, including neuromorphic [2] and high-bandwidth memory [3]. However, conventional memory technologies, such as dynamic random access memory, have limitations, including slow response times, high power consumption, and insufficient flexibility for simulating the complex adaptive processes of neural networks [4]. Ferroelectrics have emerged as a promising alternative, offering fast switching, low power consumption, and nonvolatile data retention, making them well suited for advanced artificial intelligence semiconductor architectures [5,6]. However, traditional ferroelectrics based on perovskite structures, such as barium strontium titanate [7] and lead zirconate titanate [8], face significant challenges in commercial-scale deployment due to poor compatibility with silicon interfaces [9] and the size effect, which causes ferroelectricity to vanish in thin films [10–12].

The discovery of ferroelectricity in fluorite oxides, such as $Hf_xZr_{1-x}O_2$ [13], which exhibit scale-free polarization switchability [14], robust stability of the polar phase down to subnanometer thin layers [15], and compatibility with complementary metal-oxide-semiconductor technology [16,17], offers a potential solution to the limitations of conventional ferroelectrics. Moreover, their negligibly small domain wall energy makes them suitable for ultrahigh-density memory devices [14], representing a potential paradigm shift in information technology and artificial intelligence. However, their relatively high coercive field (E_c) [18,19] remains the biggest hurdle to their implementation in memory devices, as it imposes substantial stress on the material during operation, which can lead to device breakdown [20–22]. In recent years, most studies have focused on elemental and interstitial doping to reduce the high coercive field [23–25]. Although these approaches have successfully achieved a low E_c, the oxygen vacancies induced by dopants lower the device's endurance [26,27], motivating us to explore alternative solutions for reducing high E_c in the pristine fluorite structures.

In this manuscript, we use phonon mode engineering and first-principles simulations (see the Supplemental Material [28] for details; Refs. [29–35] are cited in the Supplemental Material) to present a mechanism for intrinsically reducing the polarization-switching energy barrier associated with E_c by selectively controlling the dynamics of soft modes. A comparative analysis of polarization-switching paths reveals that the incorporation of soft modes facilitates the transformation of intermediate states from unstable high-symmetry configurations to metastable low-symmetry phases, thereby reducing the associated energy barrier. This finding suggests that deliberately introducing soft modes along the switching pathway can serve as an effective strategy for energy barrier reduction. To demonstrate this concept, we identify symmetry-allowed catalytic couplings that enable the condensation of soft modes through group-theoretical analysis and first-principles

*These authors contributed equally to this work.
†Contact author: junhee@unist.ac.kr

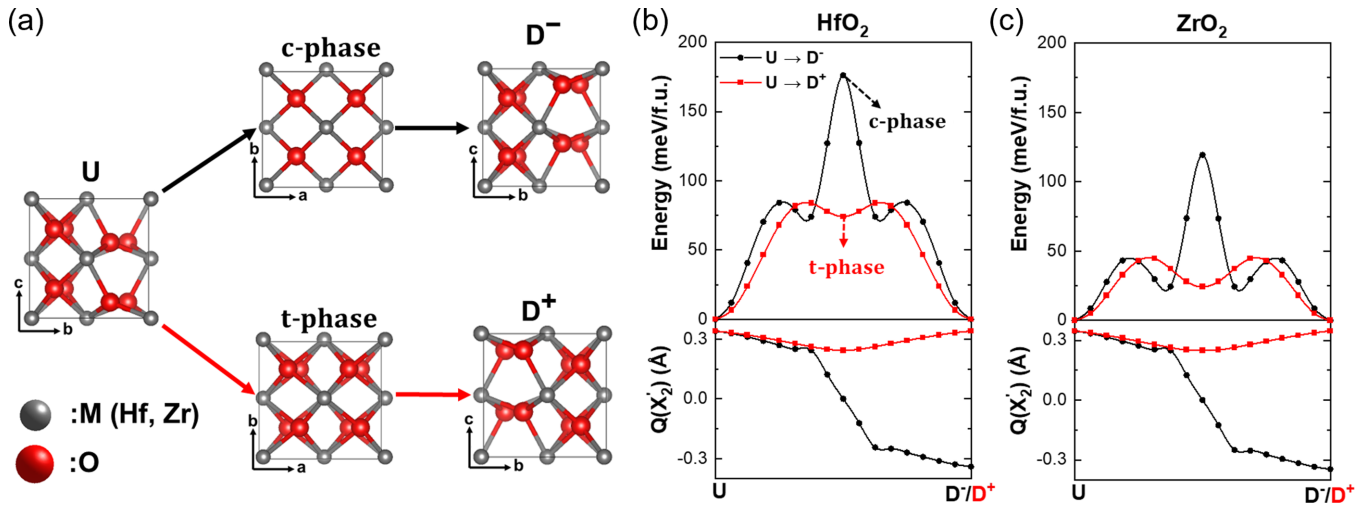

FIG. 1. (a) Two distinct pathways for polarization switching from the up-polarized (U) state to the down-polarized states (D^+ and D^-) in the o-phase HfO_2 are characterized by different intermediate phases: the U → D^- and U → D^+ paths involve c-phase and t-phase as their respective intermediate states. The energy barriers estimated from NEB calculations in HfO_2 [panel (b), top] and ZrO_2 [panel (c), top] show that the U → D^- path has a high barrier, while the U → D^+ path exhibits a significantly lower one. [(b), bottom], [(c), bottom] The soft mode X_2' reverses its sign along the U → D^- path and is suppressed at the intermediate state, leading to the formation of a c-phase, while it remains unchanged along the U → D^+ path and stays nonzero at the intermediate state, resulting in a t-phase.

calculations. Our first-principles simulations confirm that these newly activated soft modes create transition states that are energetically more favorable than the conventional states, drastically reducing the energy barrier for both Landau-type (homogeneous) and local switching. Thus, our mechanism offers an alternative strategy for lowering the coercive field in pristine fluorite ferroelectrics, beyond conventional methods such as doping and vacancy engineering.

II. RESULTS AND DISCUSSION

The condensation of six oxygen distortion modes (Γ_{15}^z, X_2', X_5^y, Y_5^z, Z_5^x, and $Z_5^{\prime y}$) and two hafnium distortion modes ($Z_5^{\prime x}$ and Y_3') (see Fig. S1 of the Supplemental Material [28]) in the reference $Fm\bar{3}m$ cubic phase (c-phase) of MO_2 [36] (where M denotes Hf and Zr) transforms it into the ferroelectric $Pca2_1$ orthorhombic phase (o-phase) [34]. Although the up-polarized o-phase (U) can switch its polarization into four symmetry-equivalent down-polarized phases [37], only two are particularly important [Fig. 1(a)] [38]. One pathway proceeds by reversing the X_2' soft mode along with the polar Γ_{15}^z and is labeled D^-; it has been observed in the most stable domain walls in MO_2 and enables ultrahigh memory density due to its scale-free ferroelectricity [14]. The other pathway, labeled D^+, switches without reversing the X_2' soft mode and is favorable for homogeneous polarization switching. We note that several other modes among the eight also reverse their signs to preserve the invariant symmetry of the phonon-phonon trilinear couplings [see Eq. (S2) of the Supplemental Material [28]], but they have a lesser effect [38]. For brevity and simplicity, we have not explicitly discussed them in our analysis.

In the U → D^- path, the X_2' mode reverses its sign and becomes zero at the transition state, resulting in a c-phase intermediate. In contrast, along the U → D^+ path, the X_2' mode retains its sign. It remains nonzero at the transition state [Fig. 1(a)], leading to a metastable t-phase intermediate state with a lower energy barrier than the former [Figs. 1(b) and 1(c)]. This suggests that the condensation of a soft mode at the transition state is crucial for reducing the switching barrier by introducing a metastable phase. Thus, it is essential to induce a soft mode at the transition state during polarization switching, particularly in pathways such as the U → D^- path, where the energy barrier is substantially increased as a result of the intrinsic instability of the intermediate structure.

Using group theory, we found that the high-frequency Γ_{25}^x mode ($\omega \simeq 600\,\mathrm{cm}^{-1}$) (see Fig. S2 of the Supplemental Material [28]), originally absent in the o-phase, can play a catalytic role in inducing a soft mode through its strong trilinear couplings with $Z_5^{\prime y}$, an existing o-phase mode, and the Z_2' soft mode, which is not inherently condensed in the o-phase [Fig. 2(a)]. Interestingly, the symmetry of the Γ_{25}^x mode also allows strong bilinear coupling with lattice shear strain ε_{yz} in both HfO_2 [Fig. 2(b)] and ZrO_2 [Fig. 2(c)]. As a result, a small external shear strain can effectively induce this high-frequency mode in the o-phase, activating its trilinear couplings and inducing the Z_2' mode. Although a shear strain exceeding 5 degrees transforms the o-phase into the most stable monoclinic $P2_1/c$ phase (m-phase) of MO_2 [35], we found that applying a 3-degree ε_{yz} remains well below this threshold and drastically reduces the energy of the transition state in both switching pathways.

Surprisingly, we found that applying a 3-degree ε_{yz} shear strain along the U → D^- Landau-type (homogeneous) switching path effectively reduces the energy barrier by lowering the energy of the transition state in both HfO_2 [Fig. 3(a)] and ZrO_2 [Fig. 3(b)] relative to the unstrained path. This reduction occurs because the additionally induced Z_2' soft mode condenses in place of the suppressed X_2' soft mode at the transition state [Figs. 3(c) and 3(d)], transforming the unstable high-symmetry c-phase into the metastable t-phase-like structure. In contrast, along the U → D^+ switching path, the

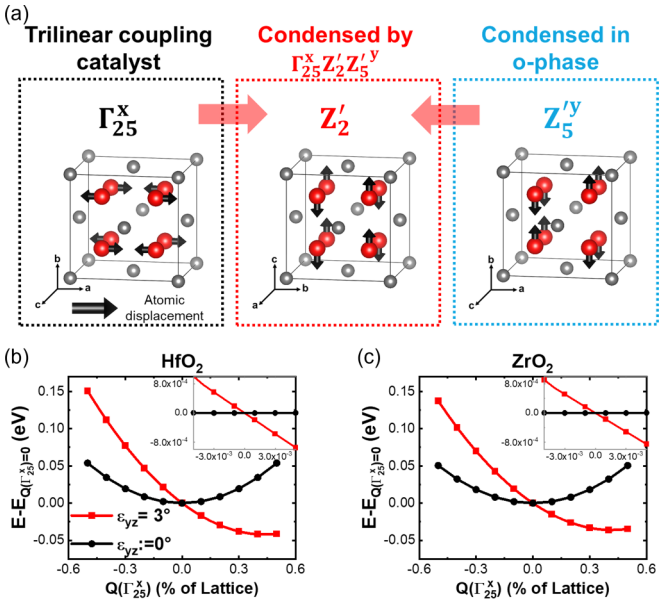

FIG. 2. (a) Atomic displacements (black arrows) of the Γ_{25}^{x} mode (induced by the application of ε_{yz} shear strain), the unstable Z_2' mode, and the o-phase mode $Z_5'^{y}$ in the unit cell of the reference c-phase. These modes exhibit strong trilinear coupling, which leads to the condensation of the Z_2' mode in the o-phase under ε_{yz} shear strain. (b), (c) Energy landscapes of the Γ_{25}^{z} mode under ε_{yz} shear strain in HfO_2 and ZrO_2, confirming their bilinear coupling, as the even symmetry of the energy landscape without strain (black line) is broken under shear strain (red line).

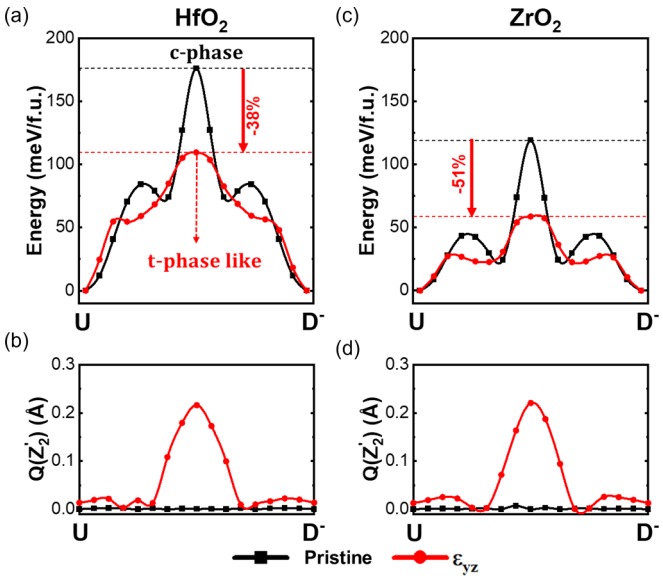

FIG. 3. The energy barriers estimated by NEB calculations along the U → D$^-$ path in pristine HfO_2 [panel (a)] and ZrO_2 [panel (b)] are shown by black lines, and those under 3-degree ε_{yz} shear strain are shown by red lines. The energy barrier is significantly reduced due to the applied shear strain. The amplitude of the Z_2' mode at each image along the polarization-switching path confirms that this mode is not induced in pristine HfO_2 and ZrO_2, but emerges at the intermediate phase under 3-degree shear strain, transforming the intermediate state from a c-phase (in pristine) into a metastable t-phase-like structure.

energy reduction of the transition state under the same shear strain is negligible for both HfO_2 and ZrO_2 (see Fig. S3 of the Supplemental Material [28]). This is because only one soft mode can dominate at the transition state. Since the X_2' mode is not suppressed along this path, the additionally induced Z_2' mode remains negligible at the transition state. Moreover, no bilinear or trilinear couplings are allowed between Γ_{25}^{x}, ε_{yz}, and X_2', which could otherwise lower the energy of the transition state. As a result, the influence of the Γ_{25}^{x} mode on the U → D$^+$ switching pathway's transition state is significantly weak.

Unlike Γ_{25}^{x}, which directly forms a trilinear coupling with the o-phase modes and successfully activates the Z_2' soft mode, the degenerate counterparts Γ_{25}^{y} and Γ_{25}^{z} do not exhibit trilinear couplings with any o-phase modes that could activate soft modes. However, we found that Γ_{25}^{y} exhibits a trilinear coupling with Z_2' and $Z_5'^{x}$. Although $Z_5'^{x}$ (an oxygen mode) is not condensed in the o-phase, it can be induced through a strain-phonon trilinear coupling of the form $\varepsilon_{xz}Z_5'^{x}Z_5'^{y}$. Consequently, ε_{xz} can also induce the Z_2' mode at the transition state and reduce the energy barrier along the U → D$^-$ switching path (see Fig. S4 of the Supplemental Material [28]), similar to ε_{yz}. In contrast, Γ_{25}^{z}, which emerges due to ε_{xy} shear strain, does not exhibit any direct or indirect coupling capable of condensing a soft mode at the transition state. Therefore, it does not reduce the energy barrier along the U → D$^-$ Landau-type switching paths (see Fig. S4 of the Supplemental Material [28]). We also found that the emergence of Γ_{25}^{α} ($\alpha = x, y, z$) due to their respective shear strains $\varepsilon_{\beta\gamma}$ ($\beta < \gamma \neq \alpha$) has a relatively small effect on reducing the energy barrier along the U → D$^+$ Landau-type switching paths (see Fig. S3 of the Supplemental Material [28]). In this case, the X_2' soft mode dominates at the transition state, and its coupling with Γ_{25}^{α} primarily leads to the condensation of other high-frequency modes, which do not significantly contribute to lowering the energy barrier.

After a successful attempt to reduce the energy barrier in Landau-type switching, we further analyze the local polarization-switching path between U/D$^-$ domain wall structures, which are referred to be the ultrahigh memory density [14]. To verify the effect of soft mode manifestation induced by ε_{yz} shear strain on reducing the energy barrier of the local polarization-switching path, we compute the local switching domain wall structures in HfO_2 [Fig. 4(a)] and ZrO_2 [Fig. 4(b)] under 3-degree ε_{yz} shear strain, showing stable domain wall structures and remnant polarization values similar to the pristine state, indicating well-preserved unique properties of fluorite ferroelectrics [14]. We further perform NEB calculations [39] on the local nucleation [Figs. 4(c) and 4(d)] and domain propagation after nucleation [Figs. 4(e) and 4(f)] in both materials with and without 3-degree ε_{yz} shear strain applied, confirming effective reductions in the energy barrier of the local polarization-switching path, particularly up to 52% in HfO_2. These results show that under applied shear strain, the energy of the intermediate state during the switching process is significantly lowered compared to the pristine state, drastically influencing energy reduction.

To determine the cause of this energy reduction, we perform phonon decomposition of the intermediate states of each

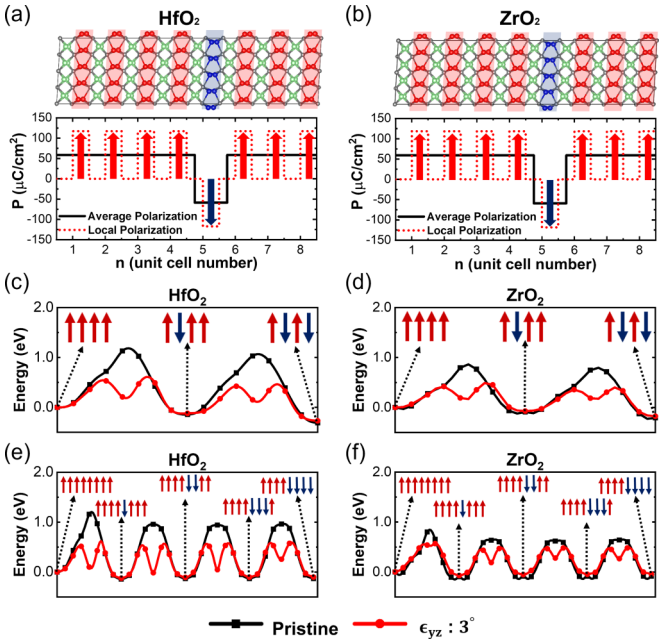

FIG. 4. (a), (b) Stable domain wall structures and local polarization characteristics are preserved in HfO_2 and ZrO_2 fluorites under a 3-degree ε_{yz} shear strain. Comparing the path with applied shear strain (red line) to the pristine path without strain (black line) in panels (c)–(f) shows that the shear strain significantly lowers the energy barriers for nucleation [panels (c) and (d)] and propagation [panels (e) and (f)]. This indicates that, through mode-catalyzed stabilization, the local polarization-switching path can be promoted as the dominant switching pathway.

material [Figs. 5(a) and 5(b)]. Unlike the pristine intermediate state, which has a structure similar to the c-phase, the phonon decomposition reveals that the intermediate state under ε_{yz} shear strain shows the m-phase-like structure, a known stable fluorite phase. In general, for the same switching path, the intermediate state remains the same in both homogeneous and local switching. Surprisingly, under ε_{yz} shear strain, the U $\rightarrow$ D^- switching path in homogeneous switching exhibits a t-phase-like intermediate state, while local switching shows an m-phase-like one. This difference arises because, in homogeneous switching, the stable modes that do not change sign [see Fig. S1(b) of the Supplemental Material [28]] during the process are suppressed to zero at the transition state, leaving only the unstable Z_2' mode nonzero, which leads to t-phase-like structure. In contrast, during local switching, these stable modes that do not reverse their signs remain nonzero due to their coupling with adjacent, unswitched unit cells. Notably, these modes are common in the m-phase [see Fig. S5(c) of the Supplemental Material [28]], which leads to the stabilization of an m-phase-like intermediate state during local switching in U/D^- domain wall structure. This phenomenon occurs more strongly in HfO_2 than in ZrO_2, contributing to the highly stable intermediate state of HfO_2. Interestingly, a similar m-phase-like structure has also been observed at the transition state along unconventional switching pathways [40]. However, in those cases, the oxygen atoms migrate across the Hf plane in a direction opposite to the electric field, which ultimately limits the response time [41]. In contrast, our proposed mechanism confines the oxygen displacement within the metal plane, allowing for a faster response and eliminating

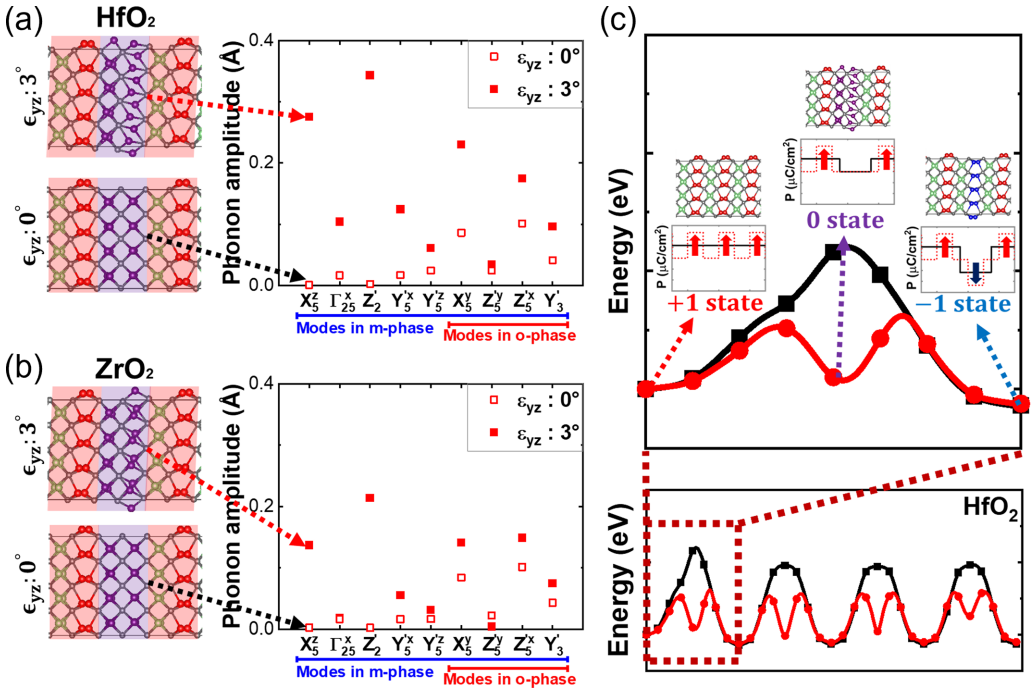

FIG. 5. (a), (b) In the absence of strain, the intermediate structure resembles the unstable $Fm\bar{3}m$ phase. Upon applying ε_{yz} shear strain, the induced Γ_{25}^x and Z_2' modes, along with distortions from the neighboring o-phase ($Pca2_1$), transform the intermediate state into a metastable structure similar to the $P2_1/c$ phase, resulting in a reduced energy barrier. (c) The stabilization of this intermediate state provides additional information states, highlighting the potential of fluorites as intrinsic ternary logic devices.

the need for oxygen migration outside the fluorite framework, thereby reducing the likelihood of defect formation, such as oxygen vacancies.

Moreover, the metastable intermediate structure induced by soft mode manifestation provides additional information states for semiconductor device operation, demonstrating the potential of fluorite as an intrinsic ternary logic material [Fig. 5(c)] [42,43]. This phenomenon opens the possibility of fluorite ferroelectrics serving as a multibit memory material, establishing it as a robust next-generation memory material. We further analyze the effect of ε_{xy} shear strain on local switching and find that, although this strain activates the Z_2' soft mode, NEB calculations show that this shear strain produces an energy barrier comparable to that of the pristine case (see Fig. S5 of the Supplemental Material [28]). This is because, unlike ε_{yz}, the ε_{xz} strain and Z_2' mode are not symmetrically capable of inducing the m-phase modes at the transition state. As a result, the energy of the intermediate state remains high, and the overall energy barrier does not decrease under ε_{xy} shear strain.

In summary, we have demonstrated that the manifestation of soft modes can reduce the energy barriers of polarization-switching paths in fluorite ferroelectrics. Unlike the conventional methods of reducing the coercive field using dopants, this approach avoids side effects that compromise device properties, such as oxygen vacancies. We have demonstrated the ability to selectively lower the energy barriers of specific switching paths based on the induced soft mode under shear strain in homogeneous and local switching. Importantly, we found that ε_{yz} facilitates local polarization switching in the most stable domain wall structures, while ε_{xy} and ε_{zx} have no significant effect. This unique characteristic allows us to selectively circumvent the energy barriers of minor switching paths with high energy barriers, like the local polarization-switching path, making it the primary path.

We hope that this study provides an approach to solving the highly coercive field problem that has hindered the commercial application of fluorite ferroelectrics and further plays a significant role in fully leveraging the intrinsic property of high information density that, while theoretically proposed, has faced challenges in practical realization. Furthermore, we believe that our scheme can provide valuable insights into studies of surface defects to stabilize ferroelectricity in thin films [44,45], where locally broken symmetry can be linked to alterations in phonon mode frequencies, which eventually affect the polarization-switching barrier in ferroelectric materials.

ACKNOWLEDGMENTS

This work was supported by Basic Research Laboratory (RS-2023-00218799), Nano & Material Technology Development Program (RS-2024-00404361), RS-2023-00257666, and RS-2025-24535610 through the National Research Foundation of Korea (NRF) funded by the Korea government (MSIT). This work was also supported by Industrial Technology Innovation Program (RS-2025-06642983) and the Korea Institute for Advancement of Technology (KIAT) grant funded by the Korea Government (MOTIE) (P0023703, HRD Program for Industrial Innovation) and the National Supercomputing Center with supercomputing resources including technical support (KSC-2022-CRE-0075, KSC2022-CRE-0454, KSC-2022-CRE-0456, KSC-2023-CRE-0547, KSC-2024-CRE-0545).

DATA AVAILABILITY

The data supporting this study's findings are available within the article.

[1] G. Lauhoff, R. Sinha, and W. Imaino, Storage infrastructure in the AI era using tape, HDD, and NAND flash memory, IEEE Trans. Magn. **61**, 3100106 (2025).

[2] A. Basu, J. Acharya, T. Karnik, H. Liu, H. Li, J.-S. Seo, and C. Song, Low-power, adaptive neuromorphic systems: Recent progress and future directions, IEEE J. Emerg. Sel. Top. Circuits Syst. **8**, 6 (2018).

[3] S. Li, M.-S. Lin, W.-C. Chen, and C.-C. Tsai, High-bandwidth chiplet interconnects for advanced packaging technologies in AI/ML applications: Challenges and solutions, IEEE Open J. Solid-State Circuits Soc. **4**, 351 (2024).

[4] K. Yu, S. Kim, and J. R. Choi, Trends and challenges in computing-in-memory for neural network model: A review from device design to application-side optimization, IEEE Access **12**, 186679 (2024).

[5] A. Keshavarzi and W. van den Hoek, Edge intelligence—On the challenging road to a trillion smart connected IoT devices, IEEE Des. Test **36**, 41 (2019).

[6] A. Keshavarzi, K. Ni, W. Van Den Hoek, S. Datta, and A. Raychowdhury, Ferroelectronics for edge intelligence, IEEE Micro **40**, 33 (2020).

[7] C. Tan, H. Wu, M. Zhao, X. Jili, L. Yang, L. Gao, and Z. Wang, Gate-switchable BST ferroelectric MoS_2 FETs for non-volatile digital memory and analog memristor, Adv. Funct. Mater. **34**, 2405293 (2024).

[8] C.-P. Yeh, M. Lisker, B. Kalkofen, and E. P. Burte, Fabrication and investigation of three-dimensional ferroelectric capacitors for the application of Feram, AIP Adv. **6**, 035128 (2016).

[9] C.-U. Pinnow and T. Mikolajick, Material aspects in emerging nonvolatile memories, J. Electrochem. Soc. **151**, K13 (2004).

[10] T. M. Shaw, S. Trolier-McKinstry, and P. C. McIntyre, The properties of ferroelectric films at small dimensions, Annu. Rev. Mater. Res. **30**, 263 (2000).

[11] M. Yashima, T. Hoshina, D. Ishimura, S. Kobayashi, W. Nakamura, T. Tsurumi, and S. Wada, Size effect on the crystal structure of barium titanate nanoparticles, J. Appl. Phys. **98**, 014313 (2005).

[12] R. R. Mehta, B. D. Silverman, and J. T. Jacobs, Depolarization fields in thin ferroelectric films, J. Appl. Phys. **44**, 3379 (1973).

[13] T. S. Böscke, J. Müller, D. Bräuhaus, U. Schröder, and U. Böttger, Ferroelectricity in hafnium oxide thin films, Appl. Phys. Lett. **99**, 102903 (2011).

[14] H.-J. Lee, M. Lee, K. Lee, J. Jo, H. Yang, Y. Kim, S. C. Chae, U. Waghmare, and J. H. Lee, Scale-free ferroelectricity induced by flat phonon bands in HfO_2, Science **369**, 1343 (2020).

[15] S. S. Cheema *et al.*, Ultrathin ferroic HfO_2-ZrO_2 superlattice gate stack for advanced transistors, Nature (London) **604**, 65 (2022).

[16] T. Mikolajick, S. Slesazeck, M. H. Park, and U. Schroeder, Ferroelectric hafnium oxide for ferroelectric random-access memories and ferroelectric field-effect transistors, MRS Bull. **43**, 340 (2018).

[17] M.-K. Kim and J.-S. Lee, Ferroelectric analog synaptic transistors, Nano Lett. **19**, 2044 (2019).

[18] D. Zhou, Y. Guan, M. M. Vopson, J. Xu, H. Liang, F. Cao, X. Dong, J. Mueller, T. Schenk, and U. Schroeder, Electric field and temperature scaling of polarization reversal in silicon doped hafnium oxide ferroelectric thin films, Acta Mater. **99**, 240 (2015).

[19] C. Alessandri, P. Pandey, A. Abusleme, and A. Seabaugh, Switching dynamics of ferroelectric Zr-doped HfO_2, IEEE Electron Device Lett. **39**, 1780 (2018).

[20] P. Cai, H. Li, Z. Liu, T. Zhu, M. Zeng, Z. Ji, Y. Wu, A. Padovani, L. Larcher, M. Pešić, R. Wang, and R. Huang, Investigation of coercive field shift during cycling in $HfZrO_x$ ferroelectric capacitors, IEEE Trans. Electron Devices **69**, 2384 (2022).

[21] K. Toprasertpong, K. Tahara, Y. Hikosaka, K. Nakamura, H. Saito, M. Takenaka, and S. Takagi, Low operating voltage, improved breakdown tolerance, and high endurance in $Hf_{0.5}Zr_{0.5}O_2$ ferroelectric capacitors achieved by thickness scaling down to 4 nm for embedded ferroelectric memory, ACS Appl. Mater. Interfaces **14**, 51137 (2022).

[22] M. K. Lenox, S. T. Jaszewski, S. S. Fields, N. Shukla, and J. F. Ihlefeld, Impact of electric field pulse duration on ferroelectric hafnium zirconium oxide thin film capacitor endurance, Phys. Status Solidi (A) **221**, 2300566 (2024).

[23] D. Gupta, P. Kumar, and J. H. Lee, Doping engineering to reduce the coercive field of ferroelectric ZrO_2, Phys. Rev. Appl. **22**, 064039 (2024).

[24] A. G. Chernikova, M. G. Kozodaev, D. V. Negrov, E. V. Korostylev, M. H. Park, U. Schroeder, C. S. Hwang, and A. M. Markeev, Improved ferroelectric switching endurance of La-doped $Hf_{0.5}Zr_{0.5}O_2$ thin films, ACS Appl. Mater. Interfaces **10**, 2701 (2018).

[25] Y.-C. Li, T. Huang, X.-X. Li, X.-N. Zhu, D. W. Zhang, and H.-L. Lu, Domain switching characteristics in Ga-doped HfO_2 ferroelectric thin films with low coercive field, Nano Lett. **24**, 6585 (2024).

[26] X. Shao, J. Chai, F. Tian, X. Ke, M. Liao, S. Dai, H. Fan, X. Sun, H. Xu, K. Han, J. Xiang, X. Wang, J. Zhang, W. Wang, and T. Ye, Evidence of oxygen vacancy generation as physical origin of endurance fatigue of Si FeFET with $TiN/Hf_{0.5}Zr_{0.5}O_2/SiO_x/Si$ gate-stacks, IEEE Trans. Electron Devices **71**, 7461 (2024).

[27] K. Bao, J. Liao, F. Yan, S. Jia, B. Zeng, Q. Yang, M. Liao, and Y. Zhou, Enhanced endurance and imprint properties in $Hf_{0.5}Zr_{0.5}O_{2-\delta}$ ferroelectric capacitors by tailoring the oxygen vacancy, ACS Appl. Electron. Mater. **5**, 4615 (2023).

[28] See Supplemental Material at http://link.aps.org/supplemental/10.1103/kkk8-s3lk for computational methods, distortion mode analysis, and additional polarization-switching NEB results.

[29] G. Kresse and J. Furthmüller, Efficient iterative schemes for *ab initio* total-energy calculations using a plane-wave basis set, Phys. Rev. B **54**, 11169 (1996).

[30] G. Kresse and J. Furthmüller, Efficiency of *ab-initio* total energy calculations for metals and semiconductors using a plane-wave basis set, Comput. Mater. Sci. **6**, 15 (1996).

[31] J. P. Perdew, K. Burke, and M. Ernzerhof, Generalized gradient approximation made simple, Phys. Rev. Lett. **77**, 3865 (1996).

[32] G. Kresse and D. Joubert, From ultrasoft pseudopotentials to the projector augmented-wave method, Phys. Rev. B **59**, 1758 (1999).

[33] H. J. Monkhorst and J. D. Pack, Special points for Brillouin-zone integrations, Phys. Rev. B **13**, 5188 (1976).

[34] S. E. Reyes-Lillo, K. F. Garrity, and K. M. Rabe, Antiferroelectricity in thin-film ZrO_2 from first principles, Phys. Rev. B **90**, 140103 (2014).

[35] Y.-W. Chen and C. W. Liu, Effects of shear strain on HZO ferroelectric orthorhombic phases, Appl. Phys. Lett. **123**, 112901 (2023).

[36] R. Terki, G. Bertrand, H. Aourag, and C. Coddet, Cubic-to-tetragonal phase transition of HfO_2 from computational study, Mater. Lett. **62**, 1484 (2008).

[37] P. Kumar, D. Gupta, and J. H. Lee, Negative gradient energy facilitates charged domain walls in HfO_2, Phys. Rev. Lett. **134**, 166101 (2025).

[38] P. Kumar and J. H. Lee, Interface engineering for facile switching of bulk-strong polarization in Si-compatible vertical superlattices, Sci. Rep. **14**, 6811 (2024).

[39] G. Mills, H. Jónsson, and G. K. Schenter, Reversible work transition state theory: Application to dissociative adsorption of hydrogen, Surf. Sci. **324**, 305 (1995).

[40] Y. Wu, Y. Zhang, J. Jiang, L. Jiang, M. Tang, Y. Zhou, M. Liao, Q. Yang, and E. Y. Tsymbal, Unconventional polarization-switching mechanism in $(Hf, Zr)O_2$ ferroelectrics and its implications, Phys. Rev. Lett. **131**, 226802 (2023).

[41] P. Nukala, M. Ahmadi, Y. Wei, S. de Graaf, E. Stylianidis, T. Chakrabortty, S. Matzen, H. W. Zandbergen, A. Björling, D. Mannix, D. Carbone, B. Kooi, and B. Noheda, Reversible oxygen migration and phase transitions in hafnia-based ferroelectric devices, Science **372**, 630 (2021).

[42] J. W. Jeong, Y.-E. Choi, W.-S. Kim, J.-H. Park, S. Kim, S. Shin, K. Lee, J. Chang, S.-J. Kim, and K. R. Kim, Tunnelling-based ternary metal–oxide–semiconductor technology, Nat. Electron. **2**, 307 (2019).

[43] J. Nam, H. Lee, M. Lee, and J. H. Lee, Nonvolatile balanced ternary memory based on the multiferroelectric material $GeSnTe_2$, J. Phys. Chem. Lett. **10**, 7470 (2019).

[44] A. Acosta, J. M. P. Martirez, N. Lim, J. P. Chang, and E. A. Carter, Relationship between ferroelectric polarization and stoichiometry of HfO_2 surfaces, Phys. Rev. Mater. **5**, 124417 (2021).

[45] A. Acosta, J. M. P. Martirez, N. Lim, J. P. Chang, and E. A. Carter, Effect of thickness and surface composition on the stability of polarization in ferroelectric $Hf_xZr_{1-x}O_2$ thin films, Phys. Rev. Mater. **7**, 124401 (2023).